Application and Extension of the Short-Range Order Configuration, SROC, Model in Bismuth Borate Glasses

Christina Valvi and Christos-Platon Varsamis *

Posted Date: 7 July 2025

doi: 10.20944/preprints202507.0492.v1

Keywords: Structure of ionic glasses; Quantification of the short-range order of ionic glasses; Short Range Order Configuration Model; Bismuth borate glasses

 doi:10.20944/preprints202507.0492.v1

Article

Application and Extension of the Short-Range Order Configuration, SROC, Model in Bismuth Borate Glasses

Christina Valvi and Christos-Platon Varsamis *

Applied Physics Laboratory, Faculty of Engineering, University of West Attica, 250 Thivon, 112 41 Egaleo, Attica, Greece

* Correspondence: cvars@uniwa.gr

Featured Application

The short range order (SRO) structure of bismuth borate glasses, xBi_2O_3-$(1-x)B_2O_3$ is derived by applying an augmented version of the Short Range Order Configuration (SROC) model, in the range $0 \leq x \leq 0.40$. The findings of this study can be extended to investigate the SRO structure of ionic glasses of any family with cations that act exclusively as modifiers of the glassy network.

Abstract

The quantification of the short-range order (SRO) of glassy materials remains an open challenge over the years. In particular, in borate glasses this task is further complicated by the change in the B coordination number from 3 to 4 and by the formation of superstructural units. Nevertheless, in two recent articles of our group, the SRO structure of bismuth, xBi_2O_3-$(1-x)B_2O_3$, and zinc, $xZnO$-$(1-x)B_2O_3$, borate glasses was completely resolved by two completely independent methods. The first one, for Bi-borates, involved the analysis of infrared absorption coefficient spectra into Gaussian component bands whereas the second one, for Zn-borates, the application of the Short-Range Order Configuration model (SROC), an extension of the well-known lever rule. In this article, we extend the application of the SROC model in bismuth borate glasses, in the range where Bi cations were found to act predominantly as modifiers, i.e., $0.20 \leq x \leq 0.40$. Our extension results in a modification of the originally proposed SROC model, by adding an additional node, and by defining the prerequisites for any augmented version of the model. The molar fractions of the borate units for the calculated SRO structure, in a continuous way throughout the range investigated, are in excellent agreement with existing literature data. Moreover, it is highlighted how the onset of disproportionation reactions, between borate units, can be handled in the framework of the introduced Augmented Short-Range Order Configuration model, ASROC.

Keywords: structure of ionic glasses; quantification of the short-range order of ionic glasses; short range order configuration model; bismuth borate glasses

1. Introduction

Glasses are characterized by the absence of long-range order (> 20Å, "LRO") that occurs in crystalline materials. On one hand, this lack may present several advantages, like the ability of glass formation in a continuous way within the glass forming range, in contrast to the corresponding formation of crystals that requires a specific molar ratio between their constituents. On the other, the quantification of the glass structure remains a continuous challenge and currently is in a primitive state compared to the highly developed solid-state theory of crystals [1]. In practice, the crystal structure can be completely identified by XRD diffraction studies, by exploiting the lattice periodicity, whereas, on the contrary, there is no experimental method for the complete quantification of the glass structure.

 doi:10.20944/preprints202507.0492.v1

Borate glasses constitute an attractive family of materials from both a scientific and a technological viewpoint. Actually, borate glasses are encountered in a plethora of technological applications including linear and non-linear optical glasses [2], luminescence [3], and scintillator [4] applications, laser and radiation detection [5], radiation shielding [6], supercapacitors [7], energy storage and conversion devices [8], as well as bioactive glasses [9]. From the scientific viewpoint, despite of the extensive research efforts over the years, the detailed structure of borate glasses continues to be an open and intriguing challenge. This challenge originates by a couple of peculiar factors intrinsic in borate structures. The first one is attributable to the change of the B coordination number from 3 to 4, resulting in the conversion of $B\varnothing_3$ triangular to $B\varnothing_4^-$ tetrahedral entities, upon initial addition of a network modifier to pure B_2O_3 glass (∅ denotes a bridging oxygen (BO) atom, linking two structural units). This is in contrast to other conventional glass systems, like silicate glasses, where the initial addition of a network modifier to pure SiO_2 glass depolymerizes the glassy network by the formation of non-bridging oxygen atoms (NBO). In borate glasses, the formation of NBO-containing units occurs only at higher modification levels. The second factor relies on the formation of superstructural units similar to those encountered in crystalline borates, at least up to the diborate composition. The aforementioned special features of borate glasses were firstly investigated and evidenced in the pioneering works of Krogh-Moe [10–12] and Bray and coworkers [13–15].

Nowadays, it is widely accepted that the SRO structure of borate glasses consists of a variety of triangular units, with the number of BO atoms ranging from 3 to 0, namely neutral, $B\varnothing_3$, meta, $B\varnothing_2O^-$, pyro, $B\varnothing O_2^{2-}$, and ortho, BO_3^{3-}. In addition, there are two types of borate tetrahedra, i.e., meta, $B\varnothing_4^-$, and ortho, $B\varnothing_2O_2^{3-}$. It is mentioned that meta-type triangles and tetrahedra are isomeric species and the same holds for ortho-type triangular and tetrahedral species. Thus, in principle these units can participate in high-temperature isomerization equilibria:

$$B\varnothing_2O^- \rightleftarrows B\varnothing_4^- \quad (1)$$

$$BO_3^{3-} \rightleftarrows B\varnothing_2O_2^{3-} \quad (2)$$

which, upon cooling the melt, govern the particular speciation of SRO structural units in borate glasses [16–18].

The particular borate speciation of the glass network depends strongly on the modifier content but, also, in the case of glasses having the same nominal composition, on the nature of the modifying cation. Nevertheless, despite the enormous number of research studies over the years, up to day there is no experimental technique capable to completely quantify the SRO structure of glasses. Early attempts of Kamitsos and coworkers provided a qualitative or semi quantitative analysis of the SRO structure of borate glasses by employing infrared reflectance and Raman spectroscopies [16,19–21]. Moreover, while synchronous NMR studies can provide unambiguously a quantification of the tetrahedral units population, the discrimination of the corresponding molar fractions of the various triangular units is still unresolved [22–25]. It is worthwhile noting that a detailed mapping of the borate structure can be obtained by employing classical molecular dynamics (CMD) simulations [26–29], machine-learning molecular dynamics [30] or ab-initio molecular dynamics (AIMD) studies [31,32]. All these simulations are calibrated to reproduce existing experimental data, mostly the radial distribution functions and the structure factors obtained through neutron scattering or X-ray diffraction studies, though a convincing agreement with vibrational or NMR spectra is still lacking.

Recently, we have fully resolved the SRO structure of bismuth borate glasses, xBi_2O_3-$(1-x)B_2O_3$, by a careful analysis of infrared absorption coefficient spectra into Gaussian component bands, combined with charge and mass balance considerations, as well as, the Lambert-Beer law for the integrated areas of the component bands [33]. Moreover, we also identified the SRO structure of binary zinc borate glasses, $xZnO$-$(1-x)B_2O_3$, by a completely different approach, introducing an extension of the well-known lever rule, namely the Short-Range Order Configuration model (SROC) [34]. A brief discussion of the SROC model will be presented in the next section.

While the analysis of infrared absorption coefficient spectra into Gaussian component bands can, in principle, be applied in any family of glassy materials, the unknown molar fractions of the

 doi:10.20944/preprints202507.0492.v1

structural units, along with the unknown absorption coefficients of each particular unit, may result in an underdetermined system of equations with the number of unknown parameters exceeding the number of equations. On the other hand, the application of the SROC model is always possible when the metal oxide acts exclusively as a modifier of the glass former, in the chemical viewpoint of glass formation. In the case of metal oxides that assume both a modifier and network-forming role, the SROC model cannot be applied [34].

With the above restriction in mind, this article extends the application of the SROC model in bismuth borate glasses, xBi_2O_3-$(1-x)B_2O_3$, in the $0.20 \le x \le 0.40$ range, where Bi_2O_3 acts predominantly as modifier [33]. Our extension requires a modification of the originally proposed SROC model, by adding an additional node in the composition range (see Section 3.2), resulting in an augmented version of the original model. In doing so, we also define the prerequisites and the necessary conditions for any future modified version of the SROC model. The proposed Augmented Short-Range Order Configuration model, ASROC, of this study provides the molar fractions of the borate units in a continuous way throughout the composition range investigated. Even more, it is explicitly shown how the onset of disproportionation reactions, between borate units, can be handled in the framework of the introduced ASROC model. The results for the SRO structure of the investigated glasses, in the $0.20 \le x \le 0.40$ range, are in excellent agreement with existing literature data.

2. Theoretical Background: the Lever Rule and the Short-Range Order Configuration Model

As explicitly described in the paper that introduced the SROC model [34], this model is an extension of the conventional lever rule for binary glasses. This rule says that when a modifier is introduced into the fully polymerized glass, nonbridging oxygens are created on network formers. As more modifiers are added, the creation of more nonbridging oxygens is necessitated, and so on. For the reader's convenience, in the next we will consider separately the lever rule and the SROC model.

2.1. The Conventional Lever Rule

Since pure B_2O_3 glass consists entirely of neutral borate triangles, $B\varnothing_3$, the progressive addition of a modifying metal oxide will result in the gradual transformation of neutral triangles initially into meta-type units, $B\varnothing_2O^-$ or $B\varnothing_4^-$, then into pyroborate triangles, $B\varnothing O_2^{2-}$, and, finally, into ortho-type moieties, BO_3^{3-} or $B\varnothing_2O_2^{3-}$. It is underlined that the peculiarity of the boron atom to change its coordination number from 3 to 4 results in a slight modification of the conventional lever rule. In that sense, upon initial introduction of a modifier in the fully polymerized B_2O_3 glass it is possible to create metaborate tetrahedra $B\varnothing_4^-$, where all oxygen atoms are bridging and, thus, nonbridging oxygens are absent.

The previous gradual structural transformations dictate that in the composition range of a binary glass with the chemical formula xMO-$(1-x)B_2O_3$, where M denotes a divalent cation, four **fundamental** nodes must be considered. These include the neutral, N (x=0), the meta, M (x=0.50), the pyro, P (x=0.67) and the ortho, O (x=0.75) node. Such nodes result in the partition of the composition range in three intervals, i.e., $0 \le x \le 0.50$, $0.50 \le x \le 0.67$ and $0.67 \le x \le 0.75$. According to the lever rule, in each of these intervals only two types of units can be present and, specifically the ones representing the limits of the corresponding interval. For example, in the $0.50 \le x \le 0.67$ range, between M and P nodes, the lever rule predicts that the network structure should consist only of metaborate and pyroborate entities. It is noted that the previous remarks hold also in the case of xM_2O-$(1-x)B_2O_3$ glasses, where M is a monovalent metal ion.

At this point, we should state the first two prerequisites and necessary conditions, as emerged from the lever rule:

Condition I: in the composition range four nodes are fundamental. These correspond to the neutral, N, meta, M, pyro, P, and ortho, O, nominal compositions.

 doi:10.20944/preprints202507.0492.v1

Condition II: at each interval between the fundamental nodes, only two types of structural units are allowed. These units correspond to the two fundamental nodes that define the interval.

Once the previous conditions are established, it is straightforward to calculate the corresponding molar fractions of the various borate building units, by invoking only mass and charge balance considerations. This is feasible due to condition II, since there are two equations with two unknown molar fractions. It is mentioned that in the original paper of the SROC model [34], instead of the charge conservation the equivalent representation of the ratio of oxygen atoms to boron, $A(x)$, was adopted. Denoting by X_N, X_M, X_P and X_O the molar fractions for neutral, meta, pyro and orthoborate species, respectively, the following equations are easily derived (for analytical details see [34]):

Range I $(0 \le x \le 0.50)$

$$X_N(x) = \frac{1-2x}{1-x} \quad (3a)$$

$$X_M(x) = \frac{x}{1-x} \quad (3b)$$

Range II $(0.50 \le x \le 0.67)$

$$X_M(x) = \frac{2-3x}{1-x} \quad (4a)$$

$$X_P(x) = \frac{2x-1}{1-x} \quad (4b)$$

Range III $(0.67 \le x \le 0.75)$

$$X_P(x) = \frac{3-4x}{1-x} \quad (5a)$$

$$X_O(x) = \frac{3x-2}{1-x} \quad (5b)$$

The functions $X_N(x), X_M(x), X_P(x)$ and $X_O(x)$ are depicted in Figure 1.

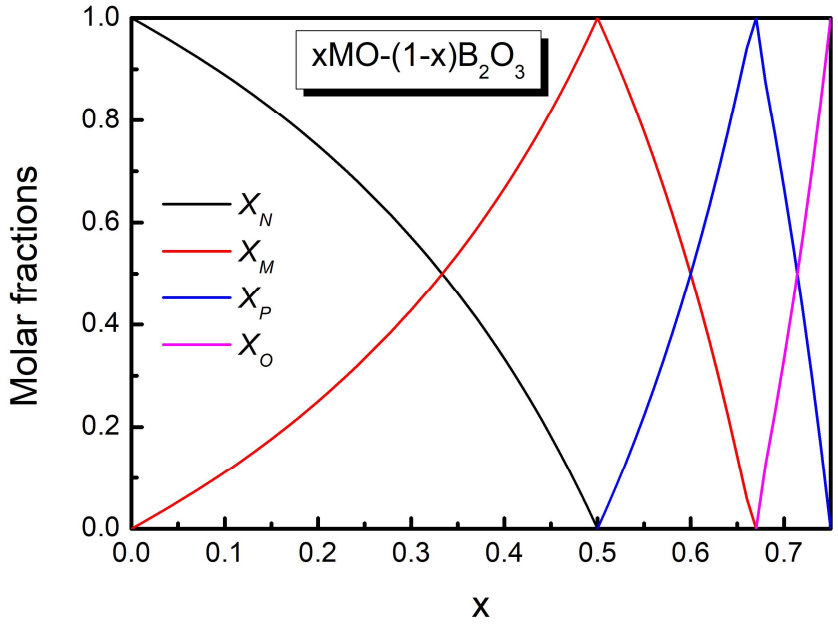

Figure 1. Molar fractions of borate units in xMO-(1-x)B_2O_3 glasses calculated by the conventional lever rule. X_N, X_M, X_P and X_O denote the corresponding molar fractions of neutral, $B\varnothing_3$, meta-type, $B\varnothing_2O^-$ or $B\varnothing_4^-$, pyro-, $B\varnothing O_2^{2-}$, and ortho-type, BO_3^{3-} or $B\varnothing_2O_2^{3-}$, units. In the composition range, x, the four fundamental nodes N (x = 0), M (x = 0.5), P (x = 0.67) and O (x = 0.75) are considered.

At this point, it is also evident that each function of the molar fractions assumes a maximum value of 1 at the corresponding node, i.e., $X_M(x) = 1$ at $x = 0.5$ (M node), and, in addition, it reaches the value 0 at the adjacent nodes, i.e., $X_M(x) = 0$ at $x = 0$ (N node) and $x = 0.67$ (P node). This observation imposes the third necessary condition for the lever rule:

 doi:10.20944/preprints202507.0492.v1

Condition III: each function of the molar fractions presents a maximum value 1 at the node that represent the particular unit and reaches 0 at the two adjacent nodes.

2.2. The Original SROC Model

According to the lever rule, the SRO structure of binary borate glasses with the same nominal composition should be identical and independent of the cation type. Unfortunately, this is not the case and the SRO structure not only exhibits a strong dependence on the cation type, but, in addition, for a particular glass composition there is clear evidence for the existence of structural units that are not predicted from the lever rule, see for example [15,16,19–21,34].

In order to resolve the previous issues, the lever rule approach was extended by assuming that the functions of Figure 1 represent the normalized contributions of the particular short-range order configurations (SROC) in binary borate glasses, xMO-(1-x)B_2O_3, with x=0 (N), x=0.5 (M), x=0.67 (P) and x=0.75 (O). Then, these functions, denoted as $X_{\underline{N}}(x), X_{\underline{M}}(x), X_{\underline{P}}(x)$ and $X_{\underline{O}}(x)$, can be used to derive the SRO structure of any intermediate glass composition. The same extension is valid also in the case of xM_2O-(1-x)B_2O_3 glasses, where M is a monovalent metal ion.

To further formulate the SROC model, a mathematical formalism was adopted starting from a 5-dimensional vector space, where the fundamental basis is the set of the short-range order building units, denoted as B_j, where j is the number of bridging oxygen atoms per boron atom ($j = 0,1,2,3,4$). For example, within this notation B_4 represents a metaborate tetrahedron, B$\emptyset_4^-$, and B_0 an orthoborate triangle, BO_3^{3-}. It is underlined that this formalism does not account for the presence of orthoborate tetrahedra, B$\emptyset_2O_2^{3-}$, since in the original study there was no experimental evidence for their presence in the structure of the binary zinc borate glasses investigated. Nevertheless, an extension to a 6-dimensional vector space, including also the possible presence of orthoborate tetrahedra, is straightforward.

With the above formalism, for a particular composition of a fundamental node, i.e., the metaborate one, M, with x=0.50 and $X_{\underline{M}}(0.50) = 1$, the SROC, M, is, in general, a linear combination of the borate species B_j:

$$\underline{M} = \sum_{j=0}^{4} f_{\underline{M},j} B_j = f_{\underline{M},0} B_0 + f_{\underline{M},1} B_1 + f_{\underline{M},2} B_2 + f_{\underline{M},3} B_3 + f_{\underline{M},4} B_4 \quad (6)$$

where $f_{\underline{M},j}$ denotes the components of the M vector in the B_j basis. Equivalently, we can represent the vector M with its components, $\underline{M} = (f_{\underline{M},0}, f_{\underline{M},1}, f_{\underline{M},2}, f_{\underline{M},3}, f_{\underline{M},4})$. We observe that $\sum_{j=0}^{4} f_{\underline{x},j} = 1$, for any fundamental node X, and that the components $f_{\underline{M},j}$ coincide with the molar fractions of the borate units for the glass having the metaborate composition.

As a starting point, it is clear that for x=0 the corresponding SROC, N, consists exclusively of neutral borate triangles, B$\emptyset_3$, or in vector notation $\underline{N} = (0,0,0,1,0)$. Then, for an intermediate composition, for example the borate glass with x=0.3, where $X_{\underline{N}} = 0.57$ and $X_{\underline{M}} = 0.43$ from Figure 1, it is assumed that the SRO structure is a linear combination of the SROCs of glasses with x=0 and x=0.5 with coefficients $X_{\underline{N}} = 0.57$ and $X_{\underline{M}} = 0.43$, respectively.

In the original SROC model, where only the fundamental nodes N, M, P and O are considered, the composition interval [0,0.75) of x is divided into 3 distinct subintervals. Specifically, we have region I with x∈ [0,0.5), region II with x∈ [0.5,0.67) and region III with x∈ [0.67,0.75). By applying condition II, we have that in region I contribute only the SROCs N and M, in region II SROCs M and P, whereas in region III SROCs P and O. With these constraints, the molar fraction of each particular borate entity B_j, $\tilde{B}_j$, can be evaluated at any value of x, with the following equations:

$$\tilde{B}_j(x) = f_{\underline{N},j} X_{\underline{N}}(x) + f_{\underline{M},j} X_{\underline{M}}(x), \text{ for } 0.0 \leq x < 0.5 \quad (7a)$$

$$\tilde{B}_j(x) = f_{\underline{M},j} X_{\underline{M}}(x) + f_{\underline{P},j} X_{\underline{P}}(x), \text{ for } 0.5 \leq x < 0.67 \quad (7b)$$

$$\tilde{B}_j(x) = f_{\underline{P},j} X_{\underline{P}}(x) + f_{\underline{O},j} X_{\underline{O}}(x), \text{ for } 0.67 \leq x < 0.75 \quad (7c)$$

In the framework of the original SROC model the only input needed is the specific borate speciation for the meta-, pyro- and ortho-borate glass compositions. Alternatively, if the SRO structure of meta-, pyro- and ortho-borate glass compositions are known from existing experimental or theoretical investigations then the array of $f_{q,j}$ values, for each borate unit j within each SROC q,

 doi:10.20944/preprints202507.0492.v1

where $q \in \{\underline{N}, \underline{M}, \underline{P}, \underline{O}\}$, is known. Then, the set of Equations (7) permits a direct evaluation of the SRO structure of any glass composition. Further details are reported in Ref. [34].

2.3. Comments on the SROC Model

The original SROC model, presented in section 2.2, was capable to describe the SRO structure of the binary $xZnO\text{-}(1\text{-}x)B_2O_3$ glasses, in their, rather narrow, glass forming range, x=[0.54,0.7]. However, we have to modify the original SROC model in at least two cases. First, where there are no available data for the SRO structure at one or more of the three fundamental nodes, M, P or O (n.b. the N node is always known). The second case is a little bit trickier, i.e., the SROCs M, P and O are known, but the predictions of the SROC model do not agree with the experimental data for the SRO structure of glasses with intermediate compositions. This situation is encountered in the present study and will be analytically described in the forthcoming section.

Fortunately, both situations can be handled by adding additional nodes to the original SROC model, thus resulting in an augmented version of the SROC model. In the next section, we will describe in detail the procedure to insert an additional node in the SROC model that fulfills the previously reported necessary conditions I to III.

3. Results and Discussion

The main aim of the present study is to apply the SROC model in the binary system of bismuth borate glasses, $xBi_2O_3\text{-}(1\text{-}x)B_2O_3$. This is motivated by the fact that the SRO structure of these glasses is known from our previous investigation in the whole glass forming range, $0.20 \leq x \leq 0.80$ [33]. Moreover, the application of the SROC model in these glasses will reveal how the original proposed model can be further enhanced by introducing additional nodes, besides the fundamental ones, in the composition range.

3.1. The SROC Model in Bismuth Borate Glasses

Initially, we apply the SROC model in $xBi_2O_3\text{-}(1\text{-}x)B_2O_3$ glasses, in the limited composition range $0.20 \leq x \leq 0.40$. This restriction is based on our previous finding that beyond x=0.40 Bi_2O_3 assumes a dual role, both of a modifier and of a glass former, as explicitly shown in Ref. [33]. In this case, the charge balance equation, or the calculation of the O/B ratio, A(x), cannot be applied, since the exact fraction of the Bi_2O_3 acting as a modifier is unknown. So, we are left with only one equation, namely the mass balance, or, equivalently, the normalization of the two SROCs, at each subinterval of the composition range, with two unknown SROC functions.

Prior to the application of the SROC model in bismuth borates, it is underlined that two modifications are needed, with respect to $xMO\text{-}(1\text{-}x)B_2O_3$ or $xM_2O\text{-}(1\text{-}x)B_2O_3$ glasses. These changes originate from the nominal charge of Bi cations, which is +3, that modifies the charge per boron and oxygen atoms per boron functions, compared to mono- or divalent cations. More precisely, if we adopt the charge per boron function, $c(x)$, for mono- or divalent cations, we have:

$$c(x) = \frac{2x}{2(1-x)} = \frac{x}{1-x} \qquad (8a)$$

whereas, for trivalent cations, like Bi^{3+}, we get:

$$c(x) = \frac{6x}{2(1-x)} = \frac{3x}{1-x} \qquad (8b)$$

The first modification is reflected in the actual value in the composition range of the three fundamental nodes M, P and O, with respect to $xMO\text{-}(1\text{-}x)B_2O_3$ or $xM_2O\text{-}(1\text{-}x)B_2O_3$ glasses. In particular, the metaborate, M, SROC node, corresponding to $c(x) = 1$, occurs at $x = 0.5$, for M^+ or M^{++} cations, and at $x = 0.25$ for Bi^{3+} ions. Along the same lines, for Bi^{3+} ions the SROC P and O nodes occur at positions $x = 0.4$ and $x = 0.5$, respectively. This is straightforward from Eq. (8b) since for P node $c(x) = 2$ and for O node $c(x) = 3$. We recall that for M^+ or M^{++} cations, SROC P and O nodes are situated at $x = 0.67$ and $x = 0.75$, respectively. Such changes affect directly the different subintervals of the composition range. In particular, in the present case we have again three intervals

 doi:10.20944/preprints202507.0492.v1

but with different limits: Region I with $x \epsilon$ [0,0.25], Region II with $x \epsilon$ [0.25,0.40] and Region III with $x \epsilon$ [0.40,0.50].

The second modification is related to the expressions of the functions $X_{\underline{N}}(x), X_{\underline{M}}(x), X_{\underline{P}}(x)$ and $X_{\underline{O}}(x)$. Following the original paper, we use the ratio of oxygen atoms to boron, $A(x)$, function. Then, for xBi_2O_3-$(1-x)B_2O_3$ glasses we have that:

$A(x) = \frac{3x+3(1-x)}{2(1-x)} = \frac{1.5}{1-x}$ (9a)

This is a different function compared to the one that applies to M^{+} or M^{++} metal ions:

$A(x) = \frac{x+3(1-x)}{2(1-x)} = \frac{1,5-x}{1-x}$ (9b)

By using the appropriate Equation (9a), the functions $X_{\underline{N}}(x), X_{\underline{M}}(x), X_{\underline{P}}(x)$ and $X_{\underline{O}}(x)$ can be easily calculated for the three new regions, in bismuth borate glasses:

Region I: $0 \leq x \leq 0.25$ (between nodes N and M)

$$X_{\underline{N}} + X_{\underline{M}} = 1$$

$1.5X_{\underline{N}} + 2X_{\underline{M}} = A(x) = \frac{1.5}{1-x}$

By solving, we get:

$X_{\underline{N}}(x) = \frac{1-4x}{1-x}$ (10a)

$X_{\underline{M}}(x) = \frac{3x}{1-x}$ (10b)

Region II: $0.25 \leq x \leq 0.40$ (between nodes M and P)

$X_{\underline{M}} + X_{\underline{P}} = 1$

$$2X_{\underline{M}} + 2.5X_{\underline{P}} = A(x) = \frac{1.5}{1-x}$$

Resulting in:

$X_{\underline{M}}(x) = \frac{2-5x}{1-x}$ (11a)

$X_{\underline{P}}(x) = \frac{4x-1}{1-x}$ (11b)

Region III: $0.40 \leq x \leq 0.50$ (between nodes P and O)

$X_{\underline{P}} + X_{\underline{O}} = 1$

$$2.5X_{\underline{P}} + 3X_{\underline{O}} = A(x) = \frac{1.5}{1-x}$$

Solving the above system gives:

$X_{\underline{P}}(x) = \frac{3-6x}{1-x}$ (12a)

$X_{\underline{O}}(x) = \frac{5x-2}{1-x}$ (12b)

A careful examination of Equations (10)-(12) shows that functions $X_{\underline{N}}(x), X_{\underline{M}}(x), X_{\underline{P}}(x)$ and $X_{\underline{O}}(x)$ satisfy the prerequisites of condition III (see Section 2.1).

The incorporation of the aforementioned modifications in the SROC model, adapted for bismuth borate glasses, are depicted in Figure 2.

 doi:10.20944/preprints202507.0492.v1

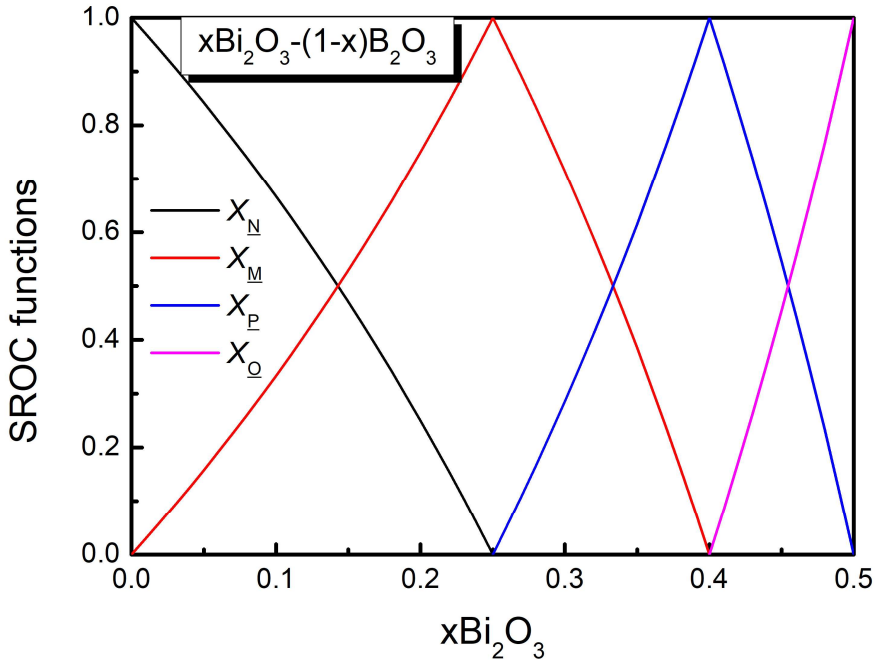

Figure 2. SROC functions in xBi_2O_3-(1-x)B_2O_3 glasses calculated by Equations (10)-(12). $X_{\underline{N}}(x), X_{\underline{M}}(x), X_{\underline{P}}(x)$ and $X_{\underline{O}}(x)$ denote the corresponding SROC functions of the four fundamental nodes N, ($x = 0$), M ($x = 0.25$), P ($x = 0.4$) and O ($x = 0.5$), respectively. For details, see text.

Finally, Equations (7) for the molar fraction of each particular borate entity B_j, $\tilde{B}_j$, at any value of x can be replaced with the following equations:

$\tilde{B}_j(x) = f_{\underline{N},j} X_{\underline{N}}(x) + f_{\underline{M},j} X_{\underline{M}}(x)$, for 0.0≤ x <0.25 (13a)

$\tilde{B}_j(x) = f_{\underline{M},j} X_{\underline{M}}(x) + f_{\underline{P},j} X_{\underline{P}}(x)$, for 0.25≤ x <0.40 (13b)

Now, it is possible to apply the SROC model in bismuth borate glasses in the range $0 \le x \le 0.40$. It is mentioned that the extension to x=0 is straightforward, though the first glass composition examined in our previous study was x=0.20 [33]. Following the approach described in Section 2.2, the only input that we need is the knowledge of the SRO structure in the three fundamental nodes N, M and P, or, equivalently, in glasses with x=0, x=0.25 and x=0.40. The orthoborate SROC O is not considered since it is beyond the upper limit of the composition range under consideration.

The structure of pure borate glass B_2O_3 consists of neutral triangles and in our previous study we analyzed the SRO structure of glasses with x=0.20, x=0.30 and x=0.40, in the range of interest [33]. The results for the molar fractions of the borate building units are summarized in Table 1.

Table 1. Molar fractions of the borate building units in xBi_2O_3-(1-x)B_2O_3 glasses, for x=0.20, x=0.30 and x=0.40. X_3, X_4, X_2, X_1 and X_0 denote the molar fractions of $B\varnothing_3$, $B\varnothing_4^-$, $B\varnothing_2O^-$, $B\varnothing O_2^{2-}$ and BO_3^{3-} units, respectively. For details see Ref.[33].

x	X_3	X_4	X_2	X_1	X_0
0.20	0.250	0.330	0.420	-	-
0.30	-	0.408	0.306	0.286	-
0.40	-	0.430		0.140	0.430

From Table 1, it is observed that the SRO structure for the glass corresponding to the M node, with x=0.25, is missing. Nevertheless, the SROC model, Equations (10) or Figure 2, predicts that for x=0.20 we have $X_{\underline{N}}(0.2) = 0.25$ and $X_{\underline{M}}(0.2) = 0.75$. These predictions are in perfect agreement with

 doi:10.20944/preprints202507.0492.v1

the data reported in Table 1, recalling that $X_{\underline{M}}(0.2)$ is equivalent to $X_4 + X_2$. On these grounds, it is reasonable to follow the predictions of the SROC model for the SRO structure of the x=0.25 glass. Thus, for x=0.25, the $\underline{M}$ node, $X_{\underline{M}}(0.25) = 1$ and the structure should consist exclusively of metaborate type units, $B\varnothing_4^-$ and $B\varnothing_2O^-$. Their molar fractions are unknown but we can use the NMR value $X_4 = 0.37$ of Ref. [35] and, consequently, $X_2 = 0.63$, for x=0.25.

At this point, we have all the information needed for nodes $\underline{N}$, $\underline{M}$ and $\underline{P}$ and the results for the components of the corresponding SROCs, following Equation (6), are reported in Table 2.

Table 2. Components of the SROCs for nodes $\underline{N}$, $\underline{M}$ and $\underline{P}$ according to Equations (13). For details see text. The subscript $\underline{q}$ represents a SROC node and $\underline{q} \in \{\underline{N}, \underline{M}, \underline{P}\}$.

SROC	$f_{\underline{q},0}$	$f_{\underline{q},1}$	$f_{\underline{q},2}$	$f_{\underline{q},3}$	$f_{\underline{q},4}$
$\underline{N}$ $(x = 0)$	0	0	0	1	0
$\underline{M}$ $(x = 0.25)$	0	0	0.63	0	0.37
$\underline{P}$ $(x = 0.40)$	0.43	0.14	0	0	0.43

The molar fractions of the borate entities for the SRO structure of bismuth borate glasses can be easily derived by applying Equations (13a) and (13b). The results are depicted in Figure 3. In the same figure, the data from our previous experimental study are also included [33]. Inspection of Figure 3 shows that for x=0.2 and x=0.4 the SROC model agrees perfectly with the experimentally derived data, as expected. In fact, for x=0.2 this agreement has already been mentioned and served as our starting point for the SROC of the $\underline{M}$ node, while for x=0.4 the corresponding SROC $\underline{P}$ used the experimental data as input.

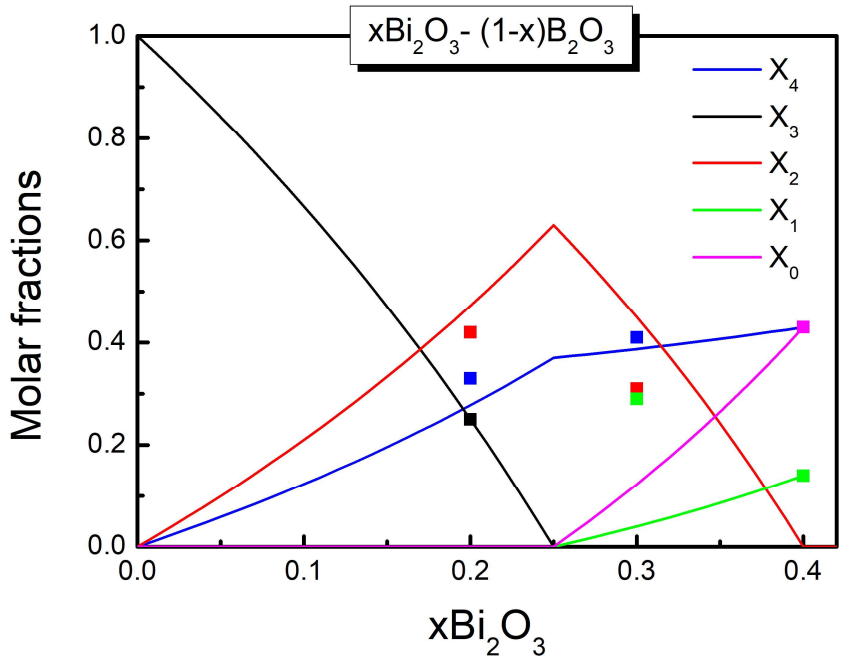

Figure 3. Molar fractions of the borate entities in xBi_2O_3-(1-x)B_2O_3 glasses, for $0 \le x \le 0.40$. Straight lines represent the fractions calculated by the original SROC model with three fundamental nodes $\underline{N}$, (x=0), $\underline{M}$, (x=0.25) and $\underline{P}$, (x=0.4). Square symbols correspond to the molar fractions derived in Ref. [33]. X_4, X_3, X_2, X_1 and X_0 denote the molar fractions of $B\varnothing_4^-$, $B\varnothing_3$, $B\varnothing_2O^-$, $B\varnothing O_2^{2-}$ and BO_3^{3-} units, respectively.

On the contrary, for the x=0.3 glass composition there is a clear divergence between the SROC model and the experimentally calculated data. The main discrepancy concerns the molar fractions of pyro- and orthoborate units. It is surprising, though, that while the SROC model predicts the presence

 doi:10.20944/preprints202507.0492.v1

of orthoborate units with a molar fraction of ca. 0.13, derived for the data in Figure 3, experimental infrared absorption coefficient spectra of the x=0.3 glass strongly suggest the absence of orthoborate triangles, as shown in Figure 3 of Ref. [33].

To trace the origin of these deviations we observe that in the SRO structure of the glass with the nominal pyroborate composition, x=0.40, pyroborate units constitute the minority species, with a molar fraction of 0.14, while metaborate tetrahedra and orthoborate units are the majority structural entities, both having a molar fraction of 0.43. This observation, which is in contrast to the stoichiometric considerations, strongly supports the occurrence of the disproportionation reaction of pyroborate units into metaborate tetrahedra and orthoborate moieties:

$2B\varnothing O_2^{2-} \rightleftarrows B\varnothing_4^- + BO_3^{3-}$ (14)

The aforementioned reaction fully explains the values of the molar fractions, reported in Table 1, for the SRO structure of the x=0.40 glass, with the nominal pyroborate stoichiometry. If we assume that initially there are only pyroborate triangles in the melt, then the onset of reaction (14) will result in equal populations of $B\varnothing_4^-$ tetrahedra and BO_3^{3-} orthoborate triangles, in agreement with their equal molar fractions of 0.43. Moreover, this value of 0.43 dictates that pyroborate units participate in this reaction with a molar fraction of 0.86, thus leaving pyroborate units with a molar fraction of 0.14 in the glass structure.

It is worthwhile noting that inspection of Table 1 evidences that the aforementioned disproportionation reaction is not active in the glass with x=0.30, since there are no orthoborate triangles in the SRO structure. In other words, the onset of reaction (14) lies somewhere in the composition range above x=0.30 and below x=0.40.

With this observation in mind, we will try to reconciliate the deviations between the original SROC model and the experimental findings by adding an additional node in the SROC model, as analytically discussed in the forthcoming section.

3.2. The Augmented SROC Model, ASROC

As previously evidenced, the SROC model cannot describe the SRO structure in bismuth borate glasses. Moreover, this weakness is probably attributed to the onset of disproportionation reaction (14) that affects directly the SRO structure of the glass and is not considered in the SROC model with the four fundamental nodes. In this section we will enhance the SROC model by inserting an additional node in order to incorporate the available experimental data of Ref. [33]. The obvious choice is the node with x=0.30, denoted as $X_{0.3}$, since the SRO structure is already known from Table 1.

First, we observe that x=0.30 lies in region II ($0.25 \le x \le 0.40$), so there is a partition of this range into two new subintervals, namely region IIa, $0.25 \le x \le 0.30$, and region IIb, $0.30 \le x \le 0.40$. In order to proceed, we observe that for x=0.30, $A(0.3) \approx 2.143$. Thus, we have the following set of equations:

Region IIa

$X_{\underline{M}} + X_{0.3} = 1$

$2X_{\underline{M}} + 2.143X_{0.3} = A(x)$

It is more instructive to express the coefficients appearing in the second equation with the values of the $A(x)$ function, that is $A(0.25) = 2$ and $A(0.3) = 2.143$. Solving the above system, we find:

$X_{\underline{M}} = \frac{A(0.3)-A(x)}{A(0.3)-A(0.25)}$ (15a)

$X_{0.3} = \frac{A(x)-A(0.25)}{A(0.3)-A(0.25)}$ (15b)

Region IIb

$X_{0.3} + X_{\underline{P}} = 1$

$2.143X_{0.3} + 2.5X_{\underline{P}} = A(x)$

Recalling that $A(0.4) = 2.5$, we get:

$X_{\underline{P}} = \frac{A(x)-A(0.3)}{A(0.4)-A(0.3)}$ (16a)

$X_{0.3} = \frac{A(0.4)-A(x)}{A(0.4)-A(0.3)}$ (16b)

 doi:10.20944/preprints202507.0492.v1

Equations (15) and (16) are quite symmetric and can be easily generalized in the case of inserting a node q between the fundamental nodes M and P. This is accomplished by replacing the term $A(0.3)$ in the above equations with the appropriate $A(q)$ value. It is easy to see that the additional node fulfills the necessary conditions II and III, as described in Section II.

The SROC functions calculated by Equations (10), (12), (15) and (16) of the augmented SROC model, ASROC, are represented in Figure 4. $X_{\underline{N}}(x), X_{\underline{M}}(x), X_{\underline{P}}(x), X_{\underline{O}}(x)$ and $X_{0.3}(x)$ denote the corresponding SROC functions of the four fundamental nodes N, (x=0), M (x=0.25), P (x=0.4), O (x=0.5) and of the new node at x=0.3, respectively.

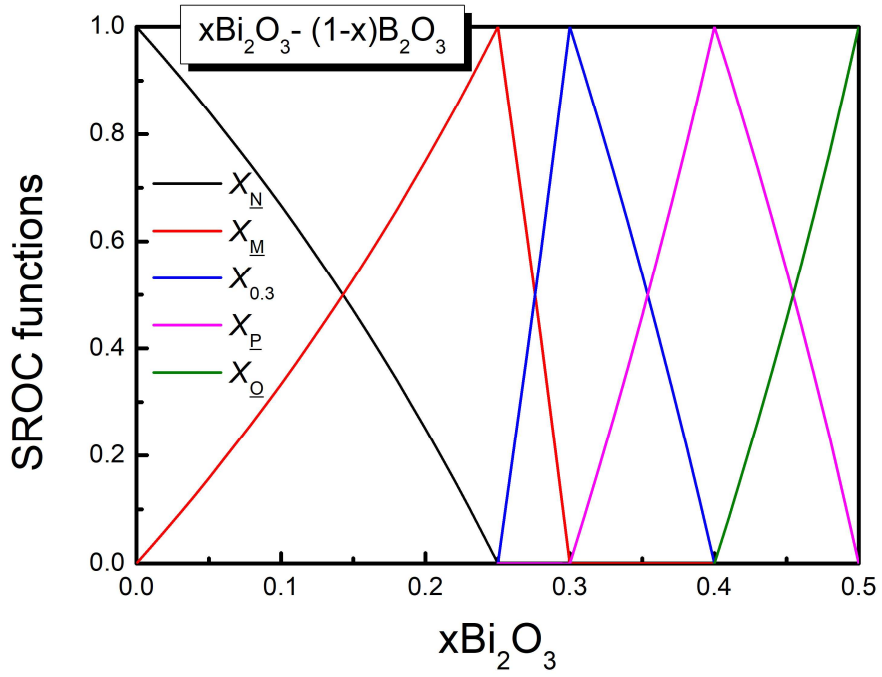

Figure 4. SROC functions in xBi_2O_3-(1-x)B_2O_3 glasses calculated by Equations (10), (12), (15) and (16). $X_{\underline{N}}(x), X_{\underline{M}}(x), X_{\underline{P}}(x), X_{\underline{O}}(x)$ and $X_{0.3}(x)$ denote the corresponding SROC functions of the four fundamental nodes N, (x=0), M (x=0.25), P (x=0.4), O (x=0.5) and of the new node at x=0.3, respectively. For details, see text.

In the framework of the ASROC model, the molar fractions of the borate entities for the SRO structure of bismuth borate glasses can be calculated by extending Equations (13a) and (13b). Since now we inserted an additional node at x=0.3, the new set of equations for the molar fraction of each particular borate entity B_j, $\tilde{B}_j$, takes the following form:

$\tilde{B}_j(x) = f_{\underline{N},j} X_{\underline{N}}(x) + f_{\underline{M},j} X_{\underline{M}}(x)$, for 0.0≤ x <0.25 (17a)

$\tilde{B}_j(x) = f_{\underline{M},j} X_{\underline{M}}(x) + f_{\underline{0.3},j} X_{\underline{0.3}}(x)$, for 0.25≤ x <0.30 (17b)

$\tilde{B}_j(x) = f_{\underline{0.3},j} X_{\underline{0.3}}(x) + f_{\underline{P},j} X_{\underline{P}}(x)$, for 0.30≤ x <0.40 (17c)

The component values $f_{\underline{q},j}$ for the SROCs N, M, 0.3, P and O are presented in Table 3. The results for the molar fractions of the borate units, derived from Equations (17a) -(17c) are depicted in Figure 5.

Table 3. Components of the SROCs for nodes N, M, 0.3 and P according to Equations (17). For details see text. The subscript q represents a SROC node and $\underline{q} \in \{\underline{N}, \underline{M}, \underline{0.3}, \underline{P}\}$.

SROC	$f_{\underline{q},0}$	$f_{\underline{q},1}$	$f_{\underline{q},2}$	$f_{\underline{q},3}$	$f_{\underline{q},4}$
N (x=0)	0	0	0	1	0

 doi:10.20944/preprints202507.0492.v1

M (x=0.25)	0	0	0.63	0	0.37
0.3 (x=0.3)	0	0.29	0.30	0	0.41
P (x=0.4)	0.43	0.14	0	0	0.43

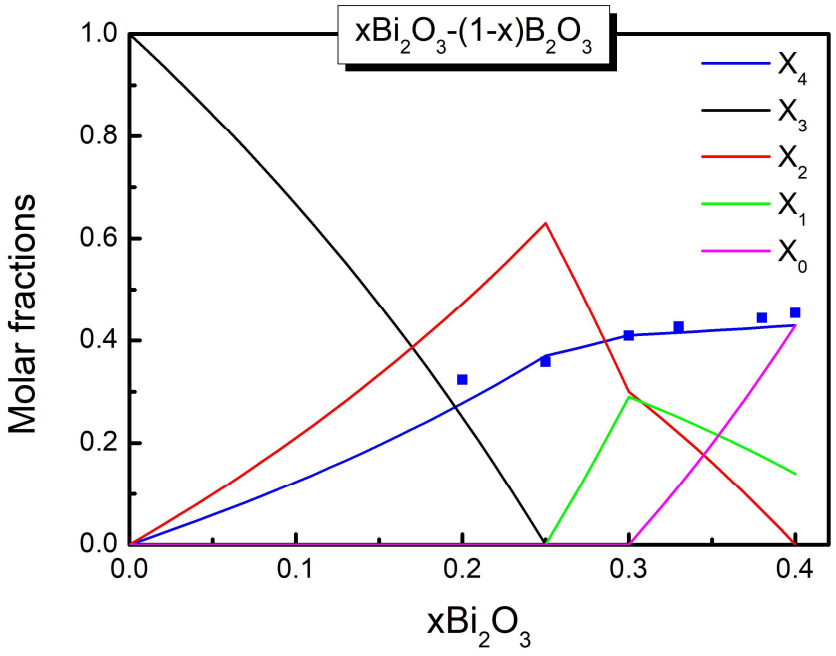

Figure 5. Molar fractions of the borate entities in xBi_2O_3-(1-x)B_2O_3 glasses, for $0 \le x \le 0.40$. Straight lines represent the fractions calculated by the augmented SROC model, ASROC with the three fundamental nodes N, (x=0), M (x=0.25), P (x=0.4) and the new node at x=0.3. X_4, X_3, X_2, X_1 and X_0 denote the molar fractions of $B\varnothing_4^-$, $B\varnothing_3$, $B\varnothing_2O^-$, $B\varnothing O_2^{2-}$ and BO_3^{3-} units, respectively. Square symbols correspond to the molar fractions of $B\varnothing_4^-$ units from the NMR study of Ref. [35].

The molar fractions of Figure 5 coincide with the experimental spectra for the SRO structure at x=0.2, x=0.3 and x=0.4 of our previous study [33] since we used this information as an input in the ASROC model. Nonetheless, it is still possible to compare our results with the available experimental data for the molar fraction of $B\varnothing_4^-$ tetrahedra from the NMR study of Ref. [35], included in Figure 5 as square symbols. As evidenced, there is an overall close agreement between the predictions of the ASROC model and the experimental NMR data. It is underlined that the ASROC model provides the molar fractions in a continuous way in the $0 \le x \le 0.40$ interval, and, more interestingly, by considering only the SRO structure of three distinct glass compositions, i.e., x=0.25, x=0.30 and x=0.40.

Another interesting trend from Figure 5 is the behavior of the molar fraction X_1 of pyroborate triangles. As shown, X_1 progressively increases after the metaborate composition at x=0.25 up to x=0.30. Then, X_1 decreases up to the pyroborate composition at x=0.40. This decrease is accompanied by a substantial increase of the population of orthoborate triangles and a slower increase of borate tetrahedra. These structural rearrangements can be fully understood by invoking the disproportionation reaction (14). Thus, the ASROC model, with the addition of only one node, incorporates the mechanism of these rearrangements.

As a final remark, it would be tempting to try to extend the model above 0.40. In order to accomplish this task first of all the nominal orthoborate node at x=0.50 has to be translated to higher composition values. Based on our previous structural findings in bismuth borate glasses [33], the glass with x=0.80 is characterized by a SRO structure of orthoborate units only. This implies that the actual position of the O node lies at x=0.80 instead of the nominal x=0.50 position. Then, the problem

 doi:10.20944/preprints202507.0492.v1

that arises is how to transform the composition interval [0.4,0.5] between the nominal positions of nodes P and O in the [0.4,0.8] interval, in order to cover the entire glass forming range of bismuth borate glasses. This subject is currently under investigation.

4. Conclusions

The Short-Range Configuration model, SROC, has been applied to investigate the structural properties of bismuth borate glasses, xBi_2O_3-$(1-x)B_2O_3$. The analysis is limited in the $0 \leq x \leq 0.40$ composition range where Bi_2O_3 acts predominantly as a modifier. In the framework of the SROC model, the SRO structure of the glasses under investigation can be derived in a continuous way throughout the entire composition range if the molar fractions of the borate building units are known, at three stoichiometric compositions. These correspond to the fundamental nodes of the model, neutral N (x=0), meta M (x=0.25) and pyro P (x=0.40).

Our analysis showed that the original SROC model, with the fundamental nodes only, fails to describe the SRO structure in bismuth borate glasses. This was attributed to the onset of a disproportionation reaction, involving pyroborate, orthoborate and tetrahedral borate units. Such a reaction affects directly the structure of the glasses and is not incorporated in the SROC model with fundamental nodes only.

The extension of the SROC model, with the addition of a new node at x=0.30, results in a successful calculation of the SRO structure of the glasses in the range under investigation. The new proposed augmented version of the SROC model, ASROC, incorporates the disproportionation reaction between the borate entities and the obtained results are in excellent agreement with existing NMR data for the molar fraction of the borate tetrahedra.

Finally, we presented and established the necessary conditions and prerequisites, initially originated from the lever rule, in order to extend the SROC model in other systems of glasses.

Author Contributions: C. Valvi; investigation, formal analysis, writing—review and editing, validation, C.P. Varsamis; conceptualization, methodology, original draft preparation, writing—review and editing, supervision. All authors have read and agreed to the published version of the manuscript.

Funding: This research received no external funding.

Abbreviations

The following abbreviations are used in this manuscript:

SROC	Short-Range Order Configuration
ASROC	Augmented Short-Range Order Configuration

References

1. Ashcroft, N.W., M., N.D. *Solid State Physics*; 1st ed.; W.B. Saunders Company: Philadelphia, 1976;
2. Santos, S.N.C.; Almeida, J.M.P.; Paula, K.T.; Tomazio, N.B.; Mastelaro, V.R.; Mendonça, C.R. Characterization of the Third-Order Optical Nonlinearity Spectrum of Barium Borate Glasses. *Opt. Mater.* **2017**, *73*, 16–19, doi:10.1016/j.optmat.2017.06.060.
3. Venkata Rao, K.; Babu, S.; Venkataiah, G.; Ratnakaram, Y.C. Optical Spectroscopy of Dy3+ Doped Borate Glasses for Luminescence Applications. *J. Mol. Struct.* **2015**, *1094*, 274–280, doi:10.1016/j.molstruc.2015.04.015.
4. Torimoto, A.; Masai, H.; Okada, G.; Kawaguchi, N.; Yanagida, T. Emission Properties of Ce-Doped Alkaline Earth Borate Glasses for Scintillator Applications. *Opt. Mater.* **2017**, *73*, 517–522, doi:10.1016/j.optmat.2017.09.006.
5. Kirdsiri, K.; Rajaramakrishna, R.; Damdee, B.; Kim, H.J.; Nuntawong, N.; Horphathum, M.; Kaewkhao, J. Influence of Alkaline Earth Oxides on Eu3+ Doped Lithium Borate Glasses for Photonic, Laser and

 doi:10.20944/preprints202507.0492.v1

Radiation Detection Material Applications. *Solid State Sci.* **2019**, *89*, 57–66, doi:10.1016/j.solidstatesciences.2018.12.019.

6. Al-Buriahi, M.S.; Sriwunkum, C.; Arslan, H.; Tonguc, B.T.; Bourham, M.A. Investigation of Barium Borate Glasses for Radiation Shielding Applications. *Appl. Phys. A* **2020**, *126*, 68, doi:10.1007/s00339-019-3254-9.
7. Khajonrit, J.; Montreeuppathum, A.; Kidkhunthod, P.; Chanlek, N.; Poo-arporn, Y.; Pinitsoontorn, S.; Maensiri, S. New Transparent Materials for Applications as Supercapacitors: Manganese-Lithium-Borate Glasses. *J. Alloys Compd.* **2018**, *763*, 199–208, doi:10.1016/j.jallcom.2018.05.300.
8. Dua, V.; Arya, S.K.; Singh, K. Review on Transition Metals Containing Lithium Borate Glasses Properties, Applications and Perspectives. *J. Mater. Sci.* **2023**, *58*, 8678–8699, doi:10.1007/s10853-023-08567-4.
9. Ege, D.; Zheng, K.; Boccaccini, A.R. Borate Bioactive Glasses (BBG): Bone Regeneration, Wound Healing Applications, and Future Directions. *ACS Appl. Bio Mater.* **2022**, *5*, 3608–3622, doi:10.1021/acsabm.2c00384.
10. Krogh-Moe, J. The Infrared Spectra of Some Vitreous and Crystalline Borates. *Arkiv Kemi* **1958**, *12*, 475–480.
11. Krogh-Moe, J. On the Structure of Boron Oxide and Alkali Borate Glasses. *Phys. Chem. Glasses* **1960**, *1*, 26–31.
12. Krogh-Moe, J. Interpretation of the Infra-Red Spectra of Boron Oxide and Alkali Borate Glasses. *Phys. Chem. Glasses* **1965**, *6*, 46–54.
13. Bray, P.J.; O'Keefe, J.G. Nuclear Magnetic Resonance Investigations of the Structure of Alkali Borate Glasses. *Phys. Chem. Glasses* **1963**, *4*, 37–46.
14. Silver, A.H.; Bray, P.J. Nuclear Magnetic Resonance Absorption in Glass. I. Nuclear Quadrupole Effects in Boron Oxide, Soda Boric Oxide, and Borosilicate Glasses. *The Journal of Chemical Physics* **1958**, *3*, 984–990.
15. Bray, P.J.; Feller, S.A.; Jellison Jr., G.E.; Yun, Y.H. B10 NMR Studies of the Structure of Borate Glasses. *Journal of Non-Crystalline Solids* **1980**, *38–39*, 93–98, doi:10.1016/0022-3093(80)90400-7.
16. Kamitsos, E.I.; Chryssikos, G.D. Borate Glass Structure by Raman and Infrared Spectroscopies. *J. Mol. Struct.* **1991**, *247*, 1–16, doi:10.1016/0022-2860(91)87058-P.
17. Varsamis, C.P.; Kamitsos, E.I.; Chryssikos, G.D. Structure of Fast-Ion-Conducting AgI-Doped Borate Glasses in Bulk and Thin Film Forms. *Phys. Rev. B* **1999**, *60*, 3885–3898, doi:10.1103/PhysRevB.60.3885.
18. Machowski, P.M.; Varsamis, C.P.E.; Kamitsos, E.I. Dependence of Sodium Borate Glass Structure on Depth from the Sample Surface. *J. Non-Cryst. Solids* **2004**, *345–346*, 213–218, doi:10.1016/j.jnoncrysol.2004.08.025.
19. Chryssikos, G.D.; Kamitsos, E.I.; Patsis, A.P.; Karakassides, M.A. On the Structure of Alkali Borate Glasses Approaching the Orthoborate Composition. *Mater. Sci. Eng. B* **1990**, *7*, 1–4, doi:10.1016/0921-5107(90)90002-S.
20. Kamitsos, E.I.; Patsis, A.P.; Karakassides, M.A.; Chryssikos, G.D. Infrared Reflectance Spectra of Lithium Borate Glasses. *J. Non-Cryst. Solids* **1990**, *126*, 52–67, doi:10.1016/0022-3093(90)91023-K.
21. Kamitsos, E.I.; Patsis, A.P.; Chryssikos, G.D. Infrared Reflectance Investigation of Alkali Diborate Glasses. *J. Non-Cryst. Solids* **1993**, *152*, 246–257, doi:10.1016/0022-3093(93)90258-Y.
22. Aguiar, P.M.; Kroeker, S. Boron Speciation and Non-Bridging Oxygens in High-Alkali Borate Glasses. *J. Non-Cryst. Solids* **2007**, *353*, 1834–1839, doi:10.1016/j.jnoncrysol.2007.02.013.
23. Montouillout, V.; Fan, H.; Del Campo, L.; Ory, S.; Rakhmatullin, A.; Fayon, F.; Malki, M. Ionic Conductivity of Lithium Borate Glasses and Local Structure Probed by High Resolution Solid-Sate NMR. *J. Non-Cryst. Solids* **2018**, *484*, 57–64, doi:10.1016/j.jnoncrysol.2018.01.020.
24. Chatzipanagis, K.I.; Tagiara, N.S.; Kamitsos, E.I.; Barrow, N.; Slagle, I.; Wilson, R.; Greiner, T.; Jesuit, M.; Leonard, N.; Phillips, A.; et al. Structure of Lead Borate Glasses by Raman, 11B MAS, and 207Pb NMR Spectroscopies. *J. Non-Cryst. Solids* **2022**, *589*, 121660, doi:10.1016/j.jnoncrysol.2022.121660.
25. Song, L.; Wang, Y.; Zhai, T.; Sun, B.; Du, Y.; Feller, S.; Yin, W.; Xu, J.; Hannon, A.C.; Zhu, F. Revealing the Microstructure and Structural Origin of Glass-Forming Range of Magnesium Borate Glass. *Ceram. Int.* **2025**, *51*, 18966–18977, doi:10.1016/j.ceramint.2025.02.075.
26. Varsamis C.P.; Vegiri A.; Kamitsos E.I. A Molecular Dynamics Study of Li-Doped Borate Glasses. *Condens. Matter Phys.* **2001**, *4*, 119, doi:10.5488/CMP.4.1.119.
27. Varsamis, C.-P.E.; Vegiri, A.; Kamitsos, E.I. Molecular Dynamics Investigation of Lithium Borate Glasses: Local Structure and Ion Dynamics. *Phys. Rev. B* **2002**, *65*, 104203, doi:10.1103/PhysRevB.65.104203.

 doi:10.20944/preprints202507.0492.v1

28. Vegiri, A.; Varsamis, C.-P.E.; Kamitsos, E.I. Composition and Temperature Dependence of Cesium-Borate Glasses by Molecular Dynamics. *J. Chem. Phys.* **2005**, *123*, 014508, doi:10.1063/1.1943414.
29. Sahu, P.; Pente, A.A.; Singh, M.D.; Chowdhri, I.A.; Sharma, K.; Goswami, M.; Ali, Sk.M.; Shenoy, K.T.; Mohan, S. Molecular Dynamics Simulation of Amorphous SiO_2 , B_2O_3 , Na_2O–SiO_2 , Na_2O–B_2O_3 , and Na_2O–B_2O_3 –SiO_2 Glasses with Variable Compositions and with Cs_2O and SrO Dopants. *J. Phys. Chem. B* **2019**, *123*, 6290–6302, doi:10.1021/acs.jpcb.9b03026.
30. Kato, T.; Lodesani, F.; Urata, S. Boron Coordination and Three-membered Ring Formation in Sodium Borate Glasses: A Machine-learning Molecular Dynamics Study. *J. Am. Ceram. Soc.* **2024**, *107*, 2888–2900, doi:10.1111/jace.19629.
31. Ohkubo, T.; Sasaki, S.; Masuno, A.; Tsuchida, E. Ab Initio Molecular Dynamics Study of Trivalent Rare Earth Rich Borate Glasses: Structural Insights and Formation Mechanisms. *J. Phys. Chem. B* **2024**, *128*, 11800–11813, doi:10.1021/acs.jpcb.4c05039.
32. Ohkubo, T.; Urata, S.; Imamura, Y.; Taniguchi, T.; Ishioka, N.; Tanida, M.; Tsuchida, E.; Deng, L.; Du, J. Modeling the Structure and Dynamics of Lithium Borosilicate Glasses with Ab Initio Molecular Dynamics Simulations. *J. Phys. Chem. C* **2021**, *125*, 8080–8089, doi:10.1021/acs.jpcc.1c00309.
33. Varsamis, C.P.E.; Makris, N.; Valvi, C.; Kamitsos, E.I. Short-Range Structure, the Role of Bismuth and Property–Structure Correlations in Bismuth Borate Glasses. *Phys. Chem. Chem. Phys.* **2021**, *23*, 10006–10020, doi:10.1039/D1CP00301A.
34. Topper, B.; Möncke, D.; Youngman, R.E.; Valvi, C.; Kamitsos, E.I.; Varsamis, C.P.E. Zinc Borate Glasses: Properties, Structure and Modelling of the Composition-Dependence of Borate Speciation. *Phys. Chem. Chem. Phys.* **2023**, *25*, 5967–5988, doi:10.1039/D2CP05517A.
35. Bajaj, A.; Khanna, A.; Chen, B.; Longstaffe, J.G.; Zwanziger, U.-W.; Zwanziger, J.W.; Gómez, Y.; González, F. Structural Investigation of Bismuth Borate Glasses and Crystalline Phases. *J. Non-Cryst. Solids* **2009**, *355*, 45–53, doi:10.1016/j.jnoncrysol.2008.09.033.